DESCRIPTION OF THE FLOW OVER A SQUARE BASE CYLINDER AT LOW REYNOLDS NUMBERS USING THE IMMERSED BOUNDARY METHOD

Jônatas Ferreira Lacerda, jonatasflacerda@hotmail.com
Tadeu Tonheiro Rodrigues, tadeu.tonheiro@gmail.com
Faculdade de Engenharia de Ilha Solteira – UNESP; Avenida Brasil, 56, Centro, CEP:15385-000, Ilha Solteira/SP

José Luiz Gasche, gasche@dem.feis.unesp.br
Faculdade de Engenharia de Ilha Solteira – UNESP; Avenida Brasil, 56, Centro, CEP:15385-000, Ilha Solteira/SP

Abstract. *The flow over square base cylinders has been extensively studied experimental and numerically, not only due to its geometric simplicity and academic interest in phenomena as separation and vortex shedding, but also owing to its practical application in heat exchangers, flow meters, and flow over buildings, bridges and offshore platforms, among others. In this work, this problem is used to validate a numerical code based on the Finite Volume Method using staggered grid, SIMPLEC for pressure-velocity coupling, central differencing interpolation scheme, and the Immersed Boundary Method together with the Virtual Physics Method to represent de cylinder. The two-dimensional incompressible unsteady flow over a square base cylinder with inlet uniform velocity profile and free stream boundary conditions for the other boundaries was simulated for Reynolds numbers varying from 100 to 1000. The time-average pressure distribution on the cylinder surface for low Reynolds number, lift and drag coefficients, and Strouhal number for all Reynolds numbers were compared with numerical and experimental results. The results presented good agreement, showing that the Immersed Boundary method is adequate to study this kind of flow.*

Keywords*: Immersed Boundary Method, Square base cylinder, Finite Volume Method, Strouhal, Drag and Lift Coefficients*

1. INTRODUCTION

The Immersed Boundary Method (IB), initially proposed by Peskin (1972), has been used successfully for studying fluid flow in complex geometries with or without fluid-structure interaction. The basic idea of this method is the use of a fixed Eulerian grid to solve the fluid flow problem together with a Lagrangian grid to represent the necessary interfaces (liquid-gas, liquid-solid, gas-solid interfaces), which is known also as immersed boundaries. These two grids interact with each other by prescribed forces in the momentum equations.

The advantage of the IB method is that the Lagrangian grid representing an interface can be displaced by the forces acting on it while the Eulerian grid remains fixed. Therefore, the fluid flow problem can be solved without remeshing, which reduces the computational cost to solve fluid-structure interaction problems. There are several models to calculate the forces to be introduced in the momentum equation. A comprehensive review about this subject is found in Mittal and Iaccarino (2005). One of the most recent models, proposed by Lima e Silva et. al. (2003), is named Virtual Physical Model (VPM) and is used in this work.

The goal of the present work is to apply de Immersed Boundary method together with the Virtual Physical model to solve the flow over a square base cylinder in order to validate a computational code based on the Finite Volume Methodology.

1.1. Flow over a square base cylinder

The flow over a square base cylinder has been extensively studied experimental and numerically not only due to its geometrical simplicity, but mainly due to the academic interest in phenomena as separation and vortex shedding. In addition, there are several industrial applications involving this type of flow as heat exchangers, flow meters, and flow over buildings, bridges and offshore platforms.

For Reynolds numbers below a critical value, Re_{cr}, the flow initially separates at the trailing edges instead the leading edges, and then reattaches on the lateral surfaces of the body, (Okajima, 1982). Thus, two symmetrical vortexes growth behind the body and are known as recirculation bubbles. For Reynolds numbers larger than the critical value, a periodical vortex shedding regime, known as Von Kárman instabilities, is noticed in this type of flow. Several values for Re_{cr} are presented in the literature. Okajima (1982) has already observed the vortex shedding formation for $Re \approx 70$. A lower value ($Re_{cr} = 54$) was reported by Kelkar and Patankar (1992). Sohankar (1998) mentions that the frequency of vortex shedding is very well defined for $Re < 200$. A dimensionless parameter generally used to present this behavior is the Strouhal number, St, which is defined as follow:

$$St = \frac{fD}{U_{in}} \tag{1}$$

where f is the vortex shedding frequency. This parameter is determined by Fast Fourier Transform (FFT) of the transversal velocity signal, which is obtained using a numerical probe located at $1D$ distance from the cylinder at the center line, as illustrated in Fig. 2.

The vortex shedding regime has direct influence in the forces acting on the immersed body, and vice-versa. The longitudinal and transversal forces are represented, respectively, by the drag (C_D) and lift (C_L) coefficients, and the mean pressure distribution on the cylinder surface is represented by the mean pressure coefficient, $\overline{C_P}$, which are defined by:

$$C_D = \frac{F_x}{0.5\rho U_{in}^2 A} \tag{2}$$

$$C_L = \frac{F_y}{0.5\rho U_{in}^2 A} \tag{3}$$

$$\overline{C_P} = \frac{1}{T}\int_0^T C_P dt = \frac{1}{T}\sum\left[\left(\frac{p - p_0}{0.5\rho U_{in}^2 A}\right)\Delta t\right] \tag{4}$$

where F_x and F_y are the acting forces on the body in the x and y directions, A is the transversal area, T is the total time simulated, Δt is the time step, p is the pressure on the cylinder surface, and p_0 is a reference pressure, settled at the entrance of the domain.

Several flow configurations have been studied in the past 30 years. Okajima (1982) has studied experimental and numerically the flow over square base cylinders for Reynolds numbers varying from 70 to $2\,10^4$, for various aspect ratios. The author has observed that the Strouhal number (flow pattern) varies remarkably with the Reynolds number and aspect ratio. Davis and Moore (1982) has simulated numerically the two-dimensional flow over a square base cylinder with free stream conditions for Reynolds numbers varying from 100 to 2800 providing drag and lift coefficients results. Sohankar (1998) has also simulated numerically the flow over a square base cylinder for several angles of incidence and low Reynolds numbers ($45-200$) and has observed that the critical Reynolds number diminishes for increasing angles of incidence. Flows in confined regimes have been studied by Davis and Moore (1984), Breuer et. al. (2000), and Zou et. al. (2005). Shear flows have been studied numerically by Cheng *et.al.* (2007), Lankadasu, and Vengadesan (2008). Owing to the large amount of results in this subject flow, flow over a square base cylinder has largely been used as bechmarck to validate numerical codes and experimental setup.

In the present work, the two-dimensional unsteady incompressible flow over a square base cylinder is numerically simulated using inlet uniform velocity and free stream conditions on the other boundaries, for Reynolds numbers varying from 100 to 1000. This problem is used to validate a numerical code based on the Finite Volume Method, using a staggered grid, SIMPLEC for pressure-velocity coupling, and central differencing scheme for interpolating the convective-diffusive terms. The Immersed Boundary Method together with the Virtual Physical Model area used to represent the cylinder in the flow. The Strouhal number, the mean pressure distribution on the cylinder surface, and the drag and lift coefficients are presented for all numerical simulations and compared with experimental and numerical data.

2. MATHEMATICAL FORMULATION

The two-dimensional unsteady incompressible flow over cylinders is governed by mass conservation and Navier-Stokes equations, given by:

$$\frac{\partial u_i}{\partial x_i} = 0 \tag{5}$$

$$\frac{\partial u_i}{\partial t} + \frac{\partial\left(u_i u_j\right)}{\partial x_j} = -\frac{1}{\rho}\frac{\partial p}{\partial x_i} + \frac{\partial}{\partial x_j}\left[\frac{\mu}{\rho}\left(\frac{\partial u_i}{\partial x_j} + \frac{\partial u_j}{\partial x_i}\right)\right] + F_i \tag{6}$$

where ρ and μ are the density and dynamic viscosity of the fluid, respectively, p is the pressure, and u_i represents the velocity components. The Eulerian force density field, F_i, in Eq. (1), models the immersed boundary, being responsible to represent the body inside the flow. The Virtual Physical Model is used to calculate this force.

2.1. Virtual Physical Model (VPM)

As mentioned previously, in the IB method the interface of a solid body immersed in the flow is defined by discrete Lagrangean points. The non-slip condition on the solid surface is prescribed by Eulerian forces, F_i, in the Navier-Stokes equations, Eq. (2). In order to determine this force, the forces acting at each Lagrangian point must be calculated and distributed to the Eulerian domain. One manner to calculate this force has been proposed by Lima e Silva et. al. (2003), and is known as Virtual Physical Model.

In this model, the Lagrangean force density is obtained through a momentum balance in a fluid particle at each discrete Lagrangian point, $\vec{x}_k$, which gives the following equation:

$$\vec{f}(\vec{x}_k,t) = \underbrace{\rho\frac{\partial\vec{V}(\vec{x}_k,t)}{\partial t}}_{\vec{fa}} + \underbrace{\rho\left(\vec{V}\cdot\vec{\nabla}\right)\vec{V}(\vec{x}_k,t)}_{\vec{fi}} - \underbrace{-\mu\nabla^2\vec{V}(\vec{x}_k,t)}_{\vec{fv}} + \underbrace{\vec{\nabla}p(\vec{x}_k,t)}_{\vec{fp}} \tag{7}$$

where $\vec{fa}$, $\vec{fi}$, $\vec{fv}$ e $\vec{fp}$ represent, respectively, the acceleration, inertial, viscous and pressure forces (by unit volume) acting on the fluid particle at the interface.

All terms described in Eq. (7) must be calculated at the interface using de velocity field, $\vec{V}(\vec{x})$, and the pressure field, $p(\vec{x})$, obtained by proper interpolations from the Eulerian domain. In order to assure the non-slip and impermeability conditions, the flow velocity at the interface must be equal to the interface velocity. The acceleration term $\vec{fa}$ is calculated by $\rho\left(\vec{V}_k - \vec{V}_{fk}\right)/\Delta t$, where $\vec{V}_k$ and $\vec{V}_{fk}$ are the interface velocity and the fluid velocity at the interface, respectively, for the Lagrangian point $\vec{x}_k$. The calculations of the spatial derivatives in the other terms of Lagrangian force density are performed by Lagrange polynomials. Four auxiliary points are defined, as illustrated in Fig. 1, and the values of pressure and velocities from the Eulerian domain are interpolated at these points by the following distribution function:

$$\phi(\vec{x}_k) = \sum_i\sum_j D_{ij}\left(\left\|\vec{x}_{ij} - \vec{x}_k\right\|\right)\phi(\vec{x}_{ij}) \tag{8}$$

where ϕ represents the pressure or the velocity components, k represents the Lagrangian and auxiliary points, $\vec{x}_{ij}$ represents a volume in Eulerian domain, and D_{ij} is given by:

$$D_{ij}\left(\left\|\vec{x}_{ij} - \vec{x}_k\right\|\right) = g(r_x)\cdot g(r_y) = g\left(\frac{\left\|x_{ij} - x_k\right\|}{h_x}\right)\cdot g\left(\frac{\left\|y_{ij} - y_k\right\|}{h_y}\right) \tag{9}$$

where h_x and h_y are the dimensions of the Eulerian control volume in the x and y directions. The values of $g(r_x)$ and $g(r_y)$ are calculated by substituting r by r_x or r_y in the following function:

$$g(r) = \begin{cases} \dfrac{3-2\|r\|+\sqrt{1+4\|r\|-4\|r\|^2}}{8}, & \text{se} \quad r<1 \\ \dfrac{1}{2}-\dfrac{3-2\|2-r\|+\sqrt{1+4\|2-r\|-4\|2-r\|^2}}{8}, & \text{se} \quad 1<r<2 \\ 0, & \text{se} \quad r>2 \end{cases} \tag{10}$$

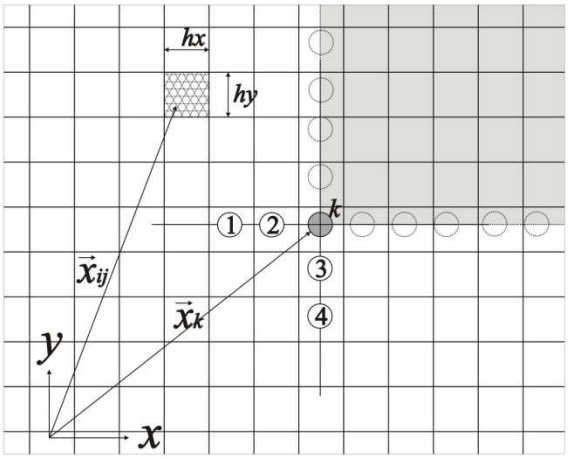

Figure 1. Lagrangian (*k*) and auxiliary (1, 2, 3, 4) points

The derivatives are then calculated by using a second order Lagrange polynomial:

$$\frac{\partial \phi}{\partial x}(x_k, y_k) = \frac{(x_k - x_2)}{(x_1 - x_2)(x_1 - x_k)}\phi_1 + \frac{(x_k - x_1)}{(x_2 - x_1)(x_2 - x_k)}\phi_2 + \frac{(x_k - x_1) + (x_k - x_2)}{(x_k - x_1)(x_k - x_2)}\phi_k \tag{11}$$

$$\frac{\partial^2 \phi}{\partial x^2}(x_k, y_k) = \frac{2\phi_1}{(x_1 - x_2)(x_1 - x_k)} + \frac{2\phi_2}{(x_2 - x_1)(x_2 - x_k)} + \frac{2\phi_{k,}}{(x_k - x_1)(x_k - x_2)} \tag{12}$$

and in the *y* direction by:

$$\frac{\partial \phi}{\partial y}(x_k, y_k) = \frac{(y_k - y_4)}{(y_3 - y_4)(y_3 - y_k)}\phi_3 + \frac{(y_k - y_3)}{(y_4 - y_3)(y_4 - y_k)}\phi_4 + \frac{(y_k - y_3) + (y_k - y_4)}{(y_k - y_3)(y_k - y_4)}\phi_k \tag{13}$$

$$\frac{\partial^2 \phi}{\partial y^2}(x_k, y_k) = \frac{2\phi_3}{(y_3 - y_4)(y_3 - y_k)} + \frac{2\phi_4}{(y_4 - y_3)(y_4 - y_k)} + \frac{2\phi_{k,}}{(y_k - y_3)(y_k - y_4)} \tag{14}$$

where ϕ_1, ϕ_2, ϕ_3 and ϕ_4 are the interpolated values obtained previously. The pairs $(x_k, y_k), (x_1, y_1)$, $(x_2, y_2), (x_3, y_3)$e (x_4, y_4) are the coordinates of the points *k*, 1, 2, 3 e 4, respectively.

The Eulerian density force field, F_i, is obtained from the Lagrangian density force, f_i, by:

$$F_i(\vec{x}_{ij}) = \sum_k D_{ij}\left(\left\|\vec{x}_{ij} - \vec{x}_k\right\|\right) f_i(\vec{x}_k)\frac{\Delta V_k}{\Delta V_{ij}} \tag{15}$$

where D_{ij} is the interpolation/distribution function defined in Eq. (5) and $\Delta V_k / \Delta V_{ij}$ is the ratio between the Lagrangian and Eulerian volumes.

Thus, a solid interface immersed in the Eulerian domain is virtually modeled by solving Eq. (2) using the density force field, F_i. This process is repeated at each time step, assuming that the mass conservation is reached. The norm L_2, defined in Eq. (16), is used to verify if the non-slip and impermeability conditions are satisfied at the interface.

$$L_2 = \frac{\sqrt{\left[\left(u_{fk} - u_k\right)^2 + \left(v_{fk} - v_k\right)^2\right]}}{N} \tag{16}$$

where *N* is the number of Lagrangian points used to represent the interface. Arruda (2004) has reached values of the order of 10^{-2} and lower values are generally considered acceptable.

3. NUMERICAL METHOD

The Finite Volume Method is used to discretize the governing equations, using a staggered grid. The central differencing scheme is used for interpolating the convective-diffusive terms and the SIMPLEC (Van Doormal and Raithby, 1984) algorithm is used to treat the pressure-velocity coupling. The algebraic equation systems are solved iteratively using the TDMA algorithm, (Thomas, 1949).

The geometry of the problem together with the boundary conditions are shown in Fig. 2.

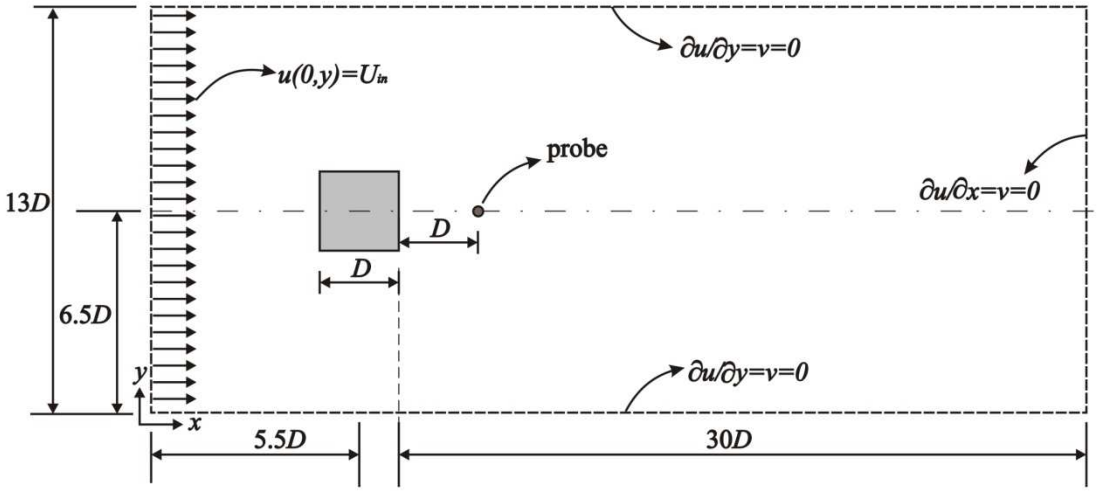

Figure 2. Geometry of the problem and boundary conditions

The computational mesh used in this work contains 148 x 90 volumes and is presented in Fig. 3. It is observed in the detail that the mesh is regular at the cylinder region.

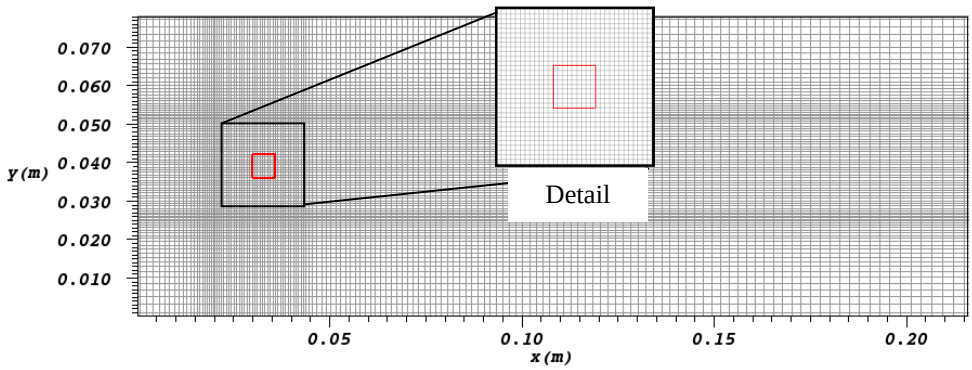

Figure 3. Computational mesh

The uniform velocity at the inlet of the flow, U_{in}, is obtained from the Reynolds number defined as :

$$Re = \frac{\rho U_{in} D}{\mu} \tag{17}$$

5. RESULTS AND DISCUSSIONS

Numerical simulations were performed for Reynolds numbers varying from 100 to 1000. The total time and the time step used in each simulation were 300 s and 10^{-2} s, respectively. Since the Reynolds number range simulated was larger than the critical value as reported by Kelkar and Patankar (1992), $Re_{cr} = 54$, in all simulated cases, the flow changes to a vortex shedding regime, known as Von Kármán street.

In Fig. 4a it is observed the formation of two recirculation bubbles behind the cylinder at the initial times for $Re = 100$. For the same Reynolds number the vortex shedding regime is observed for other times. However, for

$Re = 300$, the same behavior is not found and the vortex shedding regime occurs practically since the initial times, as shown in Fig. 4b.

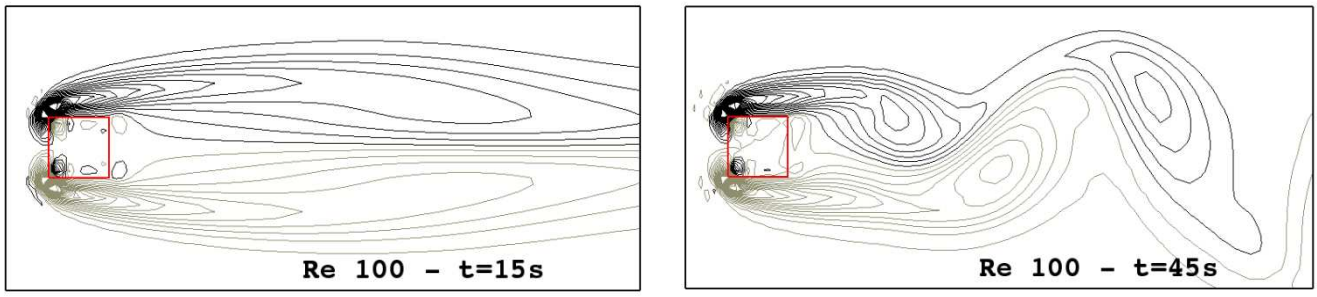

(a) *Re*=100

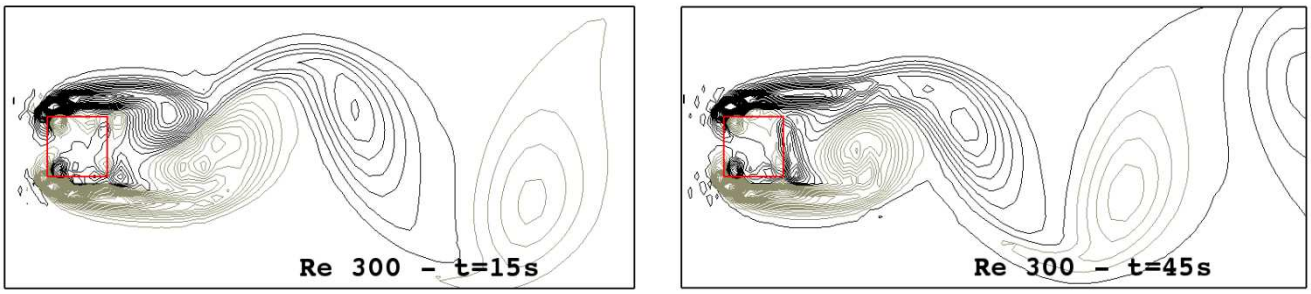

(b) *Re*=300

Figure 4. Vorticity contours at *t*=15s e 45s for (a) *Re*=100 and (b) *Re*=300

Figure 5 shows the vorticity contours at time *t*=150s for various Reynolds numbers to illustrate the vortex shedding behavior. For Reynolds equal to 100, Fig. 5.a, it is observed that the flow attaches at the lateral surface and the vortexes detach only at the trailing edges of the cylinder. However, for $Re \geq 300$ it is observed that the vortex detaches from the lateral surfaces near the leading edges of the cylinder, forming small recirculation regions on the top and bottom faces of the cylinder that are not completely steady, as mentioned in Robichaux *et. al.* (1999). Furthermore, it is observed a pairing of vortexes for $Re \geq 500$ and they stretch out in the longitudinal direction for increasing Reynolds numbers.

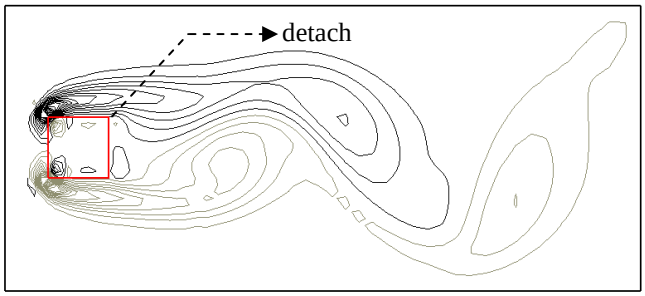

(a) *Re*=100

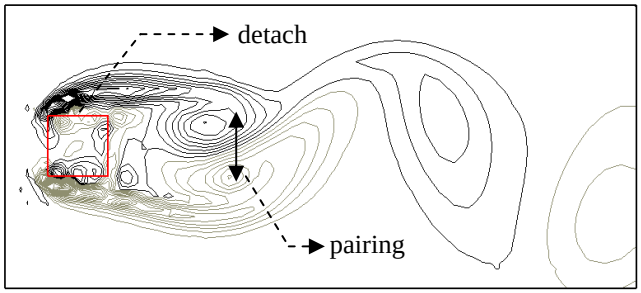

(c) *Re*=500

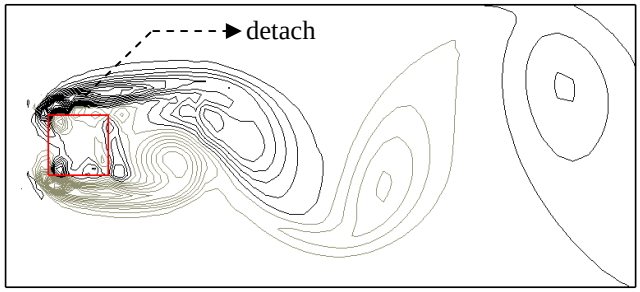

(b) *Re*=300

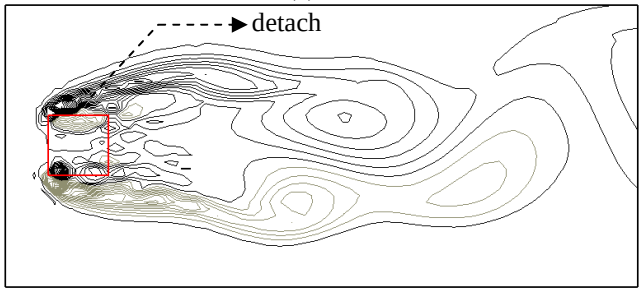

(d) *Re*=900

Figure 5. Vortex formation behind the cylinder for several *Re* at *t*= 150s

An interesting remark obtained from Fig. 5 is that there are recirculation regions inside the cylinder because, in IB method, the fluid occupies the entire domain.

Figures 6.a and 6.b show the power spectrum of the transversal velocities for Reynolds varying from 100 to 500 and 600 to 1000, respectively, highlighting the frequencies of vortex shedding used to calculate the Strouhal numbers.

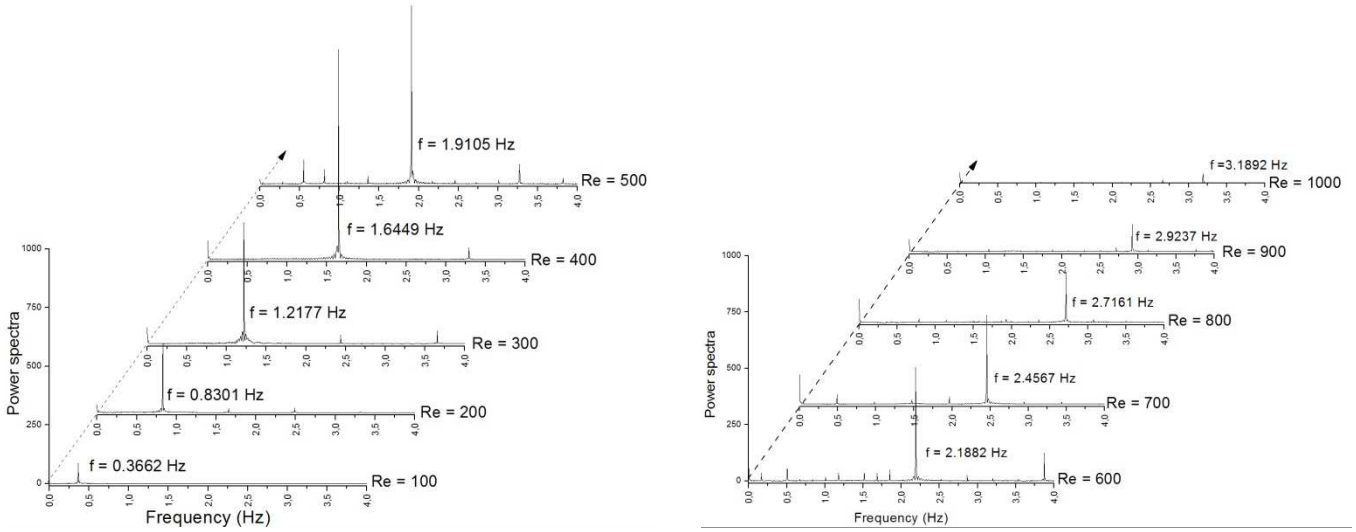

(a) *Re* 100 – 500 (b) *Re* 600 – 1000

Figure 6. Power spectra of the transversal velocity signal

The Strouhal numbers were compared with experimental data obtained by Lindquist (2000), in Fig. 7, indicating a good agreement.

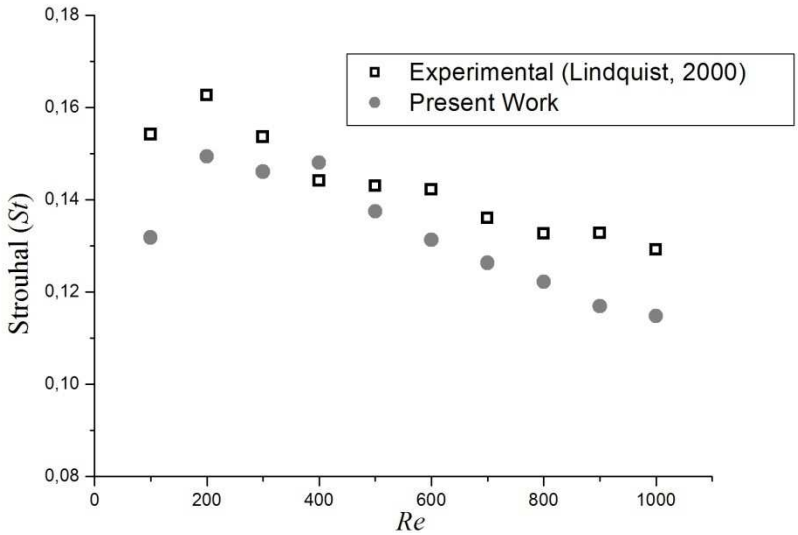

Figure 7. Strouhal number for *Re* 100 to 1000

Figure 8 shows that the mean pressure coefficient on the cylinder surface, $\overline{C_P}$, agrees satisfactorily with numerical data obtained by Cheng et. al. (2007) for Reynolds equal 100.

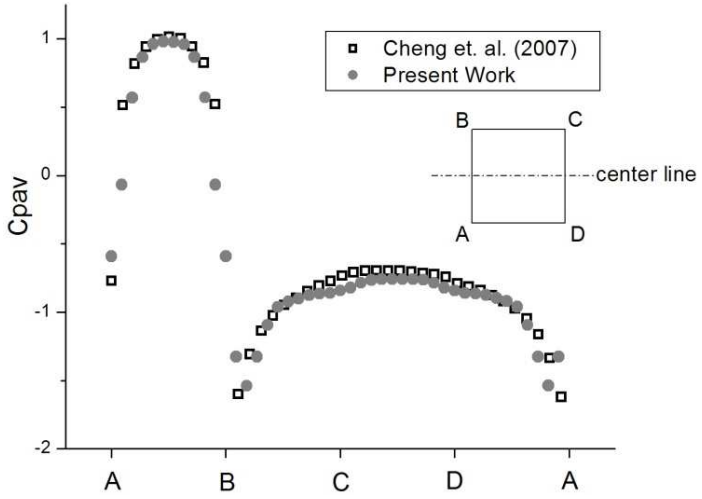

Figure 8. Mean pressure coefficient on the cylinder surface for Reynolds equal to 100

Figures 9.a and 9.b present the pressure distributions on the surfaces for all simulated Reynolds numbers. These kind of result are hardly found in the literature. It can be observed in Fig. 9a that the distribution is symmetrical in relation to the center line and the maximum value is located in the middle point of the front face AB, for $Re \leq 500$. The pressure on the lateral surfaces is larger for *Re*=100 because the vortex released at the leading edges reattaches, as observed in Fig. 5.a and mentioned in Okajima (1982). For $Re \geq 600$, Fig. 9.b, it is observed a flat pressure distribution on the frontal face. In addition, the pressure increases on the other surfaces BC, CD and AD of the cylinder for increasing Reynolds number.

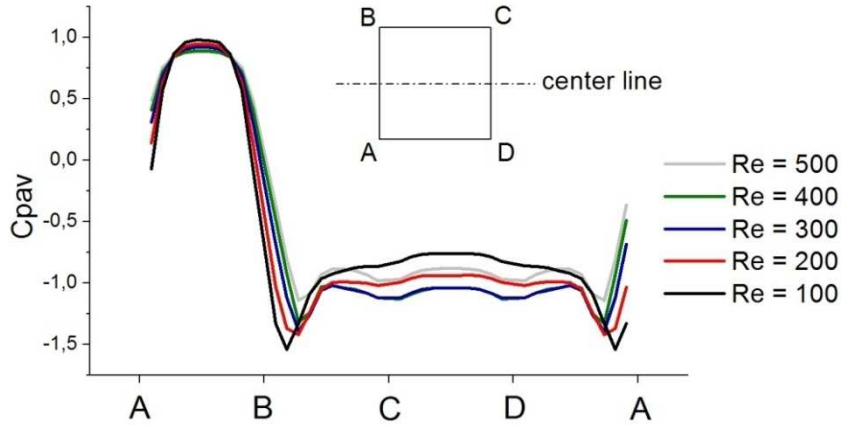

(a) *Re* 100 to 500

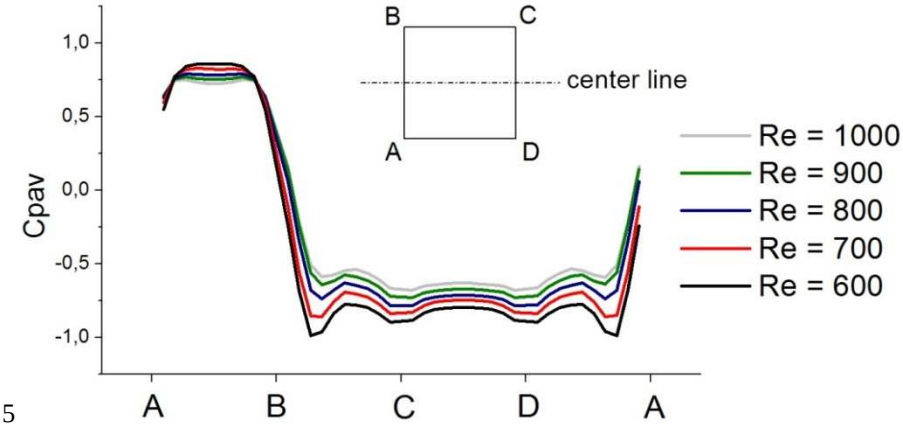

(b) *Re* 600 to 1000

Figure 9. Mean pressure coefficient on the cylinder surface for (a) *Re* 100-500 and (b) *Re* 600-1000

The behavior of the longitudinal and transversal forces acting on the cylinder are described by the drag and lift coefficients, respectively, shown in Fig. 10 for Reynolds number equal to 100, 300, and 500. For $Re < 500$, both coefficients have regular fluctuations with approximately constant amplitudes. For Re=500 the same regularity is not found because of the turbulence regime.

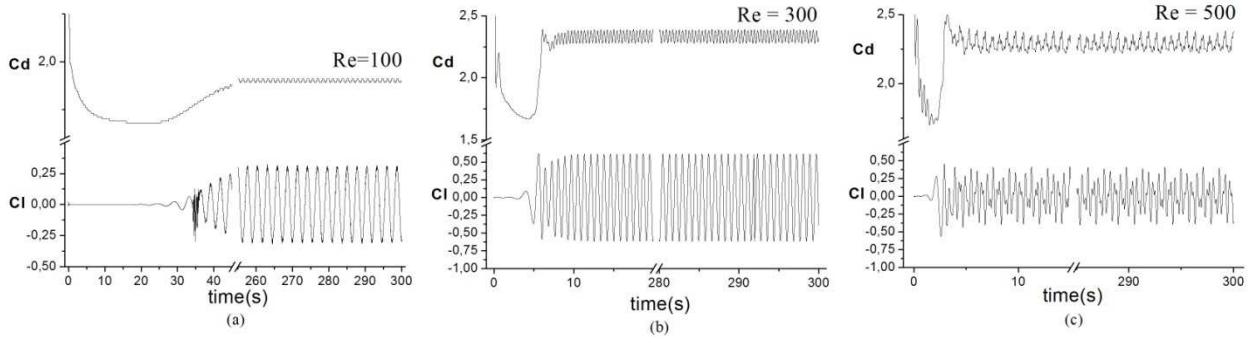

Figure 10. Drag, C_D, and lift, C_L, coefficients for *Re* equal (a) 100, (b) 300, and (c) 500

Comparisons between the results reported by other authors and the present computation for Reynolds numbers equal to 100 and 200 are given in Tab. 1, which shows good agreement mainly for the Strouhal number.

Table 1. Comparison of lift and drag coefficients and Strouhal number

	Re = 100			***Re = 200***		
	St	***Cd***	***Cl***	***St***	***Cd***	***Cl***
Okajima (1982)	0.135 – 0.14	-	-	0.140 – 0.148	1.45	-
Frank and Schonung (1990)	0.154	1.61	± 0.270	0.157	1.60	± 0.60
Kelkar and Patankar (1992)	0.130	1.80	-	-	-	-
Sohankar *et. al.* (1998)	0.146	1.47	± 0.156	0.150	1.462	± 0.377
Robichaux *et. al.* (1999)	0.154	1.53	-	0.167	2.72	-
Cheng *et. al.* (2007)	0.144	1.44	± 0.152	0.150	1.45	± 0.372
Present work	0.132	1.89	± 0.310	0.149	2.094	± 0.52

6. CONCLUSIONS

In the present work, the two-dimensional, unsteady, and incompressible flow over a square base cylinder was numerically simulated for Reynolds numbers varying from 100 to 1000. This problem was used as benchmark for validating a numerical code based on the Finite Volume Method, which uses the Immersed Boundary Method together with the Virtual Physical Method to represent the body. The comparison of the Strouhal number (*St*) and the mean pressure coefficient, $\overline{C_P}$, showed good agreement with existing experimental and numerical data. The pressure distribution on the cylinder surface for several Reynolds numbers, which is hardly found in literature, is also presented. The employed methodology was able to simulate adequately this kind of flow.

7. ACKNOWLEDGEMENTS

The authors acknowledge the financial support from FAPESP.

8. REFERENCES

Arruda, J. M., 2004, “Modelagem matemática de escoamentos internos forçados utilizando o método da fronteira imersa e o modelo físico virtual”, 146 f., tese de doutorado em Engenharia Mecânica, Universidade Federal de Uberlândia, Uberlândia, Brasil, 2004.

Breuer, M., Bernsdorf, J., Zeiser, T., Durst, F., 2000, “Accurate computations of the laminar flow past a square cylinder based on two different methods: lattice-Boltzmann and finite-volume”, International Journal of Heat and Fluid Flow, Vol. 21, pp. 186-196.

Cheng, M., Whyte, D. S., Lou, J., 2007, "Numerical simulation of flow around a square cylinder in uniform-shear flow", Journal of Fluids and Structures, Vol. 23, pp. 207-226.
Davis, R.W., Moore, E.F., 1982, "A numerical study of vortex shedding from rectangles", Journal of Fluid Mechanics, Vol. 116, pp. 475–506.
Davis, R.W., Moore, E.F., Purtell, L.P., 1984. "A numerical–experimental study of confined flow around rectangular cylinders", Physics of Fluids, Vol. 27, pp. 46–59.
Kelkar, K.M., Patankar, S.V., 1992, "Numerical prediction of vortex shedding behind square cylinders", International Journal for Numerical Methods in Fluids, Vol. 14, pp. 327-341.
Lankadasu, A., Vengadesan, S., 2008, "Onset of vortex shedding in planar shear flow past a square cylinder", International Journal of Heat and Fluid Flow, Vol. 29, pp. 1054-1059.
Lima e Silva, A.L.F., Silveira-Neto, A., Damasceno, J.J.R., 2003, "Numerical simulation of two-dimensional flows over a circular cylinder using the immersed boundary method", Journal of Computational Physics, Vol. 189, pp. 351-370.
Lindquist, C., "Estudo experimental do escoamento ao redor de cilindros de base quadrada e retangular", 188 f., dissertação de mestrado, Faculdade de Engenharia de Ilha Solteira – UNESP, Ilha Solteira, Brasil, 2000.
Mittal, R.; Iaccarino, G., 2005, "Immersed Boundary Methods", Annual Review of Fluid Mechanics, Vol. 37, pp. 239-261.
Okajima, A., 1982, "Strouhal number of rectangular cylinder", Journal of Fluid Mechanics, Vol. 123, pp. 379-398.
Patankar, S. V., 1980, "Numerical Heat Transfer and Fluid Flow", Hemisphere Publ. Corp., Washington D. C., USA, 197 p.
Peskin, C. S., 1972, "Flow patterns around heart valves: a numerical method", Journal of Computational Physics, Vol. 10, pp. 252-271.
Robichaux, J., Balachandar, S., Vanka, P.K., 1999, "Three-dimensional Floquet instability of the wake square cylinder", Physics of Fluids, Vol. 11, pp. 560-578.
Sohankar, A., Norberg, C., Davidson, L., 1998, "Low-Reynolds number flow around a square cylinder at incidence: study of blockage, onset of vortex shedding and outlet boundary condition", International Journal for Numerical Methods in Fluids, Vol. 26, pp. 39-56.
Thomas, L. H., 1949, "Elliptic Problems in Linear Difference Equations over a Network", Watson Sci. Comput. Lab. Report, Columbia University, New York, USA.
Van Doormal, J.P., Raithby, G.D., 1984, "Enhacements of the SIMPLE Method for Predicting Incompressible Fluid Flows", Numerical Heat Transfer, Vol. 7, pp. 147-163.
Zhou L., Cheng M., Hung K. C., 2005, "Suppression of fluid force on a square cylinder by flow control", Journal of Fluid and Structures, Vol. 21, pp. 151-167.

9. RESPONSIBILITY NOTICE

The authors are the only responsible for the printed material included in this paper.